Journal of Materials Research and Technology 30 (2024) 5582–5589

Contents lists available at ScienceDirect

Journal of Materials Research and Technology

journal homepage: www.elsevier.com/locate/jmrt

A novel sintering method for polycrystalline NiMnGa production for elastocaloric applications

Francesca Villa [a,b,*], Elena Villa [a], Enrico Bassani [a], Corrado Tomasi [c], Francesca Passaretti [a], Riccardo Casati [b]

[a] CNR ICMATE, Lecco Unit, Italy
[b] Politecnico di Milano, Department of Mechanical Engineering, Italy
[c] CNR ICMATE, Genova Unit, Italy

ARTICLE INFO

Keywords:
Ferromagnetic shape memory alloys
NiMnGa
Sintering
Elastocaloric effect
Microstructure
Thermoelastic martensitic transformation

ABSTRACT

NiMnGa Heusler alloy plays a key role as reference system for ferromagnetic shape memory alloys (FeSMAs) and their peculiar functional properties including large magnetic-field-induced strain, magnetocaloric and elastocaloric effects. Moreover, the microstructure of polycrystalline NiMnGa alloys has been investigated and optimized to improve the mechanical properties and to reduce their typical brittleness. For this reason, increasing interest has been devoted to different kinds of fabrication routes for this alloy, such as powder metallurgy processes. In the present study, a polycrystalline $Ni_{50}Mn_{30}Ga_{20}$ (atomic %) alloy is produced by means of an unconventional sintering method that involves the canning of powders and the subsequent processing by hot rolling. This process was implemented according to the results obtained by means of the open die pressing (ODP) sintering of NiMnGa which was investigated in a previous work. The present study is aimed at developing an alternative and cost-effective sintering method for the consolidation of fully-dense NiMnGa samples. The process allowed reducing the intrinsic brittleness of the alloy. A heat treatment at 925 °C for 6 h was applied and allowed achieving a maximum adiabatic ΔT of +6.3 °C and - 4.5 °C with a strain of 4 % and a strain rate of 400 %/min in compression. The novel method led to very promising elastocaloric properties, making NiMnGa a suitable candidate for solid-state cooling and heating applications.

1. Introduction

Among the ferromagnetic shape memory alloys (FeSMA), NiMnGa is the system which has been mostly investigated in the last 25 years. It is noticeable to consider this Heusler alloy as the main reference system for all the FeSMA and MetaSMA, (NiMnGa-, NiFeGa- or NiMnSn-based). Comprehensive studies on functional properties of NiMnGa alloy have been performed [1–4]. First, the magnetic-field-induced strain (MFIS) effects that occur thanks to the high mobility of the martensite twins that rearrange when the material is exposed to a magnetic field were studied [1,5,6] and MFIS up to 12 % were achieved in single crystals. In addition, the magnetic induction of the thermoelastic martensitic transition (TMT) to exploit the shape memory effect induced by the magnetic field was investigated. Finally, the multi-caloric properties related to the combination of the magnetocaloric and elastocaloric effect have been optimized. The caloric performances of the materials, in terms of adiabatic ΔT, have been enhanced by the application of a magnetic field and the mechanical stress required to induce the phase transformation has been decreased [7,8]. One of the critical issues that occurred throughout these investigations, preventing the practical applications, is the significant brittleness of the material [9,10]. In literature, a first attempt of hot rolling of cast NiMnGa alloy to improve ductility showed promising results [9]. Moreover, only single crystals [11–13] and melt spun ribbons [14] led to satisfactory performances in terms of caloric, magnetic, and mechanical effects, but such fabrication processes can hardly be adapted for the large-scale production. Therefore, over the years, different types of powder metallurgy and additive manufacturing processes have been developed to overcome these issues [15–24]. However, these processes still require further optimization, since the achieved densities of the NiMnGa products were lower than those of cast alloys and, in some cases, the issues related to the intrinsic brittleness were not completely solved [25]. In a previous study of some of the authors of this work, a detailed investigation about the physical properties of sintered NiMnGa alloy starting from non-spherical powders is presented [16].

* Corresponding author. CNR ICMATE, Lecco Unit, Italy.
E-mail address: francesca.villa@icmate.cnr.it (F. Villa).

https://doi.org/10.1016/j.jmrt.2024.04.259
Received 7 February 2024; Received in revised form 17 April 2024; Accepted 30 April 2024
Available online 3 May 2024
2238-7854/© 2024 The Authors. Published by Elsevier B.V. This is an open access article under the CC BY license (http://creativecommons.org/licenses/by/4.0/).

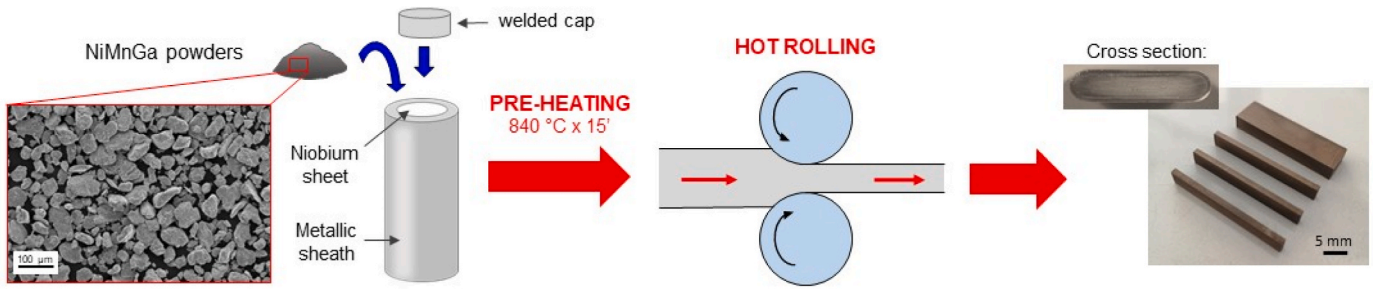

Fig. 1. Schematic of the powder consolidation procedure.

Moreover, the development of an unconventional sintering processes, i.e. the open die pressing (ODP), was carried out [26]. The ODP allowed the production of dense NiMnGa samples with enhanced mechanical properties with respect to the cast alloy and promising elastocaloric and cycling performance [27]. The NiMnGa sintered through the ODP method represents the starting point for the development of multicaloric materials, where the efficient coupling of magnetocaloric and elastocaloric effect can be exploited.

In the current work, for the first time, a *powder-in-tube* approach was followed to sinter NiMnGa powders by hot rolling. Non-spherical powders were canned and hot rolled to promote powder consolidation. The calorimetric, microstructural, and functional properties of the as-sintered and heat-treated alloy were investigated. Moreover, an evaluation of the elastocaloric performance in terms of theoretical and experimental adiabatic ΔT was carried out. Indeed, when a caloric material is subjected to an extremely rapid (adiabatic) loading, it undergoes a reversible solid-state transformation that is characterized by a latent heat which is not exchanged with the environment, leading to a material temperature increase. Upon adiabatic unloading, the material cools down due to the occurrence of the inverse transformation [28–32]. This phenomenon can be exploited for the development of solid-state cooling or heat pumping systems as sustainable alternative to the traditional vapour-based cooling systems. The elastocaloric systems are mainly applied as coolers or heat pumps at room temperature. However, it is possible to use also caloric materials that exhibit the solid-state transformation at higher or lower temperatures in order to employ them as safety or control systems that can be activated when the temperature of the environment overcomes a threshold. For NiMnGa alloy, the best elastocaloric performance in terms of adiabatic ΔT are exhibited by single crystals [33] and directionally-solidified alloys [34,35] with temperature spans up to 11.3 °C and 10.7 °C respectively. Considering NiMnGa-based alloys, e.g. NiMnGaTi [36] and NiMnGaCu [37] quaternary alloys, adiabatic ΔT up to 20 °C are achieved. The aim of this work consists in the development of new guidelines for the production of hot-rolled sintered NiMnGa FeSMA for the advancement of multicaloric materials for solid state refrigeration and heat pumping applications.

2. Materials and methods

2.1. Material processing

Cast NiMnGa ingots with nominal composition $Ni_{50}Mn_{30}Ga_{20}$ (in at. %) were produced by arc melting of pure elements (electrolytic Ni 99.97 %, electrolytic Mn 99.5 % and Ga 99.99 %) in a non-consumable electrode furnace (Leybold LK6/45). The ingots were re-melted five times. As-cast ingots were pulverized in a planetary ball mill (Fritsch Pulverisette 4) and the powders with dimensions between 50 and 100 μm were collected through calibrated sieves.

The NiMnGa powders were processed through hot rolling. The process schematic is outlined in Fig. 1. 60 g of powders were inserted into steel can with an inner diameter of 22 mm and a wall thickness of 2 mm. The can was internally coated with a thin Nb sheet that prevented the Fe diffusion from the sheath to the NiMnGa during the process. A steel plug was machined to seal the can and to leave some small channels to allow air degassing during the deformation process. The canned powder was pre-heated in a furnace at 840 °C for 15 min. Then, it was subjected to 16 steps of hot rolling that involved 1 mm of thickness reduction each. Every two steps, the can was heated up to 840 °C in the furnace for 5 min. Finally, the rolled can was cooled down by water quench and then the iron shell and niobium sheet were machined away. Bulk samples with dimensions of 40 × 30 × 6 mm^3 approximately were achieved and smaller samples with different geometries required for the various experimental tests were cut out from them by abrasive cutter. The as-produced sample was encapsulated in a quartz vial filled with Ar atmosphere and heat treated in a furnace at 925 °C for 6 h and slowly cooled down inside the furnace off.

2.2. Density, microstructural and thermo-mechanical characterization

After steel can removal, density measurements on the as-rolled sample were performed by means of the Archimedes method using a balance specifically equipped for mass measurements in air and in water. The microstructural observation was carried out on polished and chemically etched (Marble solution) samples by means of a Leitz-ARISTOMET optical microscope and the calorimetric analysis was performed through a differential scanning calorimeter DSC Q200 TA Instruments. The modulated calorimetric analysis for the measurement of the specific heat was performed by means of a temperature modulation with a period of 100 s and an amplitude of 0.5 °C over a mean value of 170 °C. The bending tests, including the dynamic thermo-mechanical analysis (DMTA) at 1 Hz frequency and low applied strain (0.02 %) and strain recovery tests at fixed applied stresses (between 0.5 and 30 MPa), were carried out with a dynamic mechanical analyzer DMA Q800 TA Instruments upon heating and cooling between 0 °C and 250 °C. The samples were cut along the rolling direction with dimensions 24 × 3.5 × 0.7 mm^3 and the instrument was equipped with a single cantilever fixture. The heating and cooling rate was set at 2 and 5 °C/min for the DMTA and strain recovery tests, respectively. By the DMTA analysis, the dissipative response of the material to the sinusoidal applied strain at fixed amplitude and frequency was investigated. This is possible through the measurement of the internal friction or $\tan(\delta)$ damping parameter which is the ratio between the loss modulus (E'') of the out-of-phase response and the storage modulus (E') of the in-phase response of the sample. During the dynamic test, the shift of the material response is quantified by the phase angle, i.e. δ. Moreover, in the complex formulation of the modulus, the ratio between the imaginary and real part of δ is given by the $\tan(\delta)$. The registered internal friction profile is the sum of different contributions. The first is the intrinsic contribution due to the material crystal structure and, in the case of the SMAs, the austenitic and martensitic phases provide different values of internal friction. A second contribution is associated with the phase transformation and is responsible for the internal friction peak in correspondence of the TMT temperatures. Finally, there is a transitory term that is typical of the measurements involving temperature spans, which depends on the

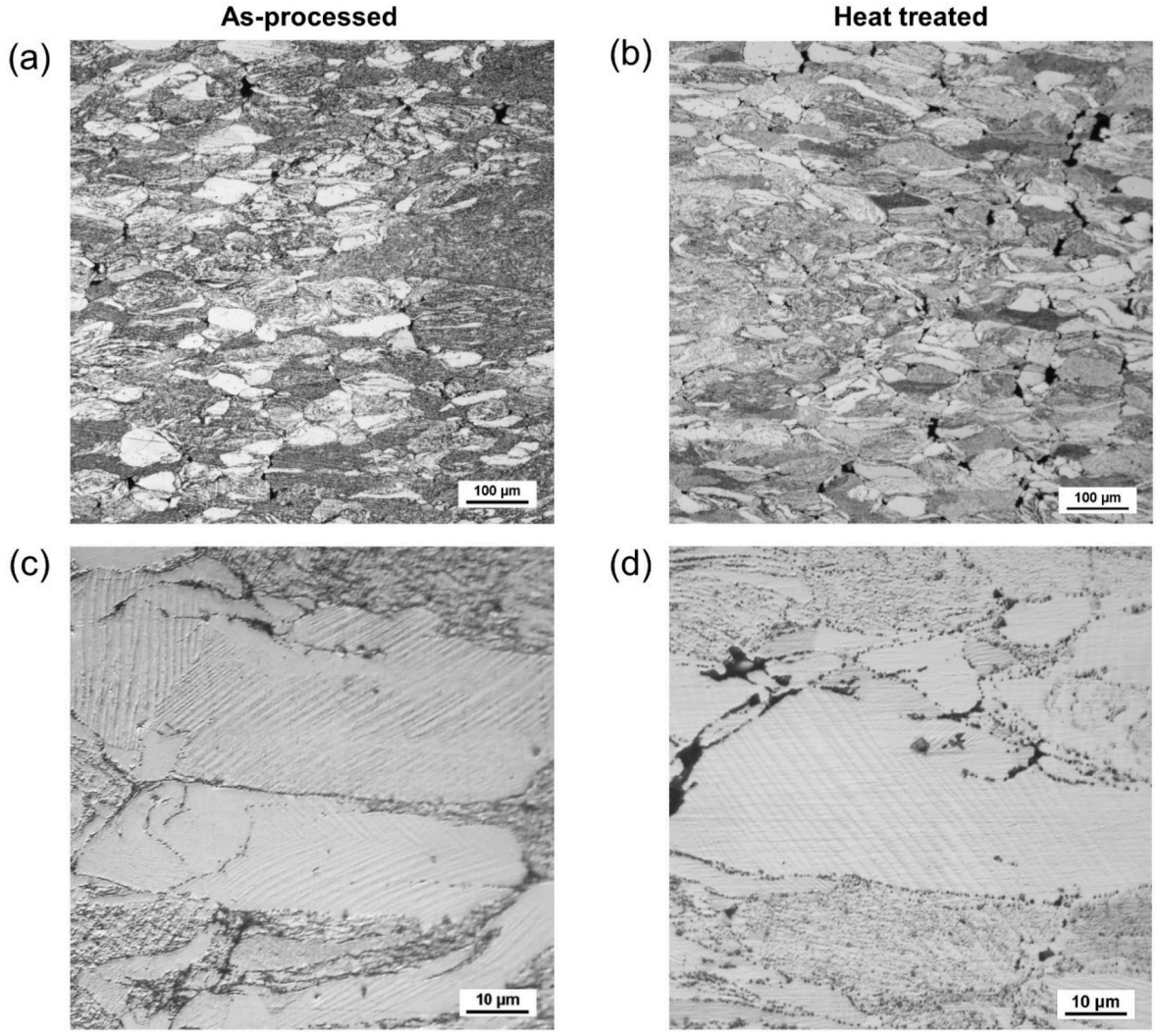

Fig. 2. Optical micrographs of NiMnGa as-processed (a and c) and heat treated (b and d) samples on etched transversal cross sections.

heating and cooling rate and on the loading frequency [38,39]. The compression tests were performed on samples with dimensions 2 × 2x5 mm^3 by means of an Instron E3000 mechanical test instrument equipped with a 3 kN load cell and a thermal chamber. In particular, the isothermal measurements were carried out at fixed temperatures (A_f, A_f + 15 °C and A_f + 35 °C) and low strain rate, i.e. 1 %/min, while the adiabatic measurements were performed at A_f + 15 °C and high strain rates (from 200 to 400 %/min). The critical stresses to induce martensite were approximatively evaluated by means of the tangent method for the determination of the slope variation of the isothermal stress-strain curves. Moreover, the temperature change of the material during the elastocaloric cycles was registered through a specific setup developed in previous studies [27,40] for the high frequency acquisition of the temperature signal through thin T-type thermocouples.

3. Results and discussion

3.1. Density, microstructural and calorimetric analysis

The compaction process allowed the production of bulk NiMnGa samples with a relative density of 97.1 % with respect to the density of the cast ingot (7.94 g/cm^3). Fig. 2(a) and (b) show low-magnification micrographs of the polished and etched transversal cross sections of the as-produced and heat treated samples. Some pores are visible in all the micrographs and their morphology reveals that in some regions

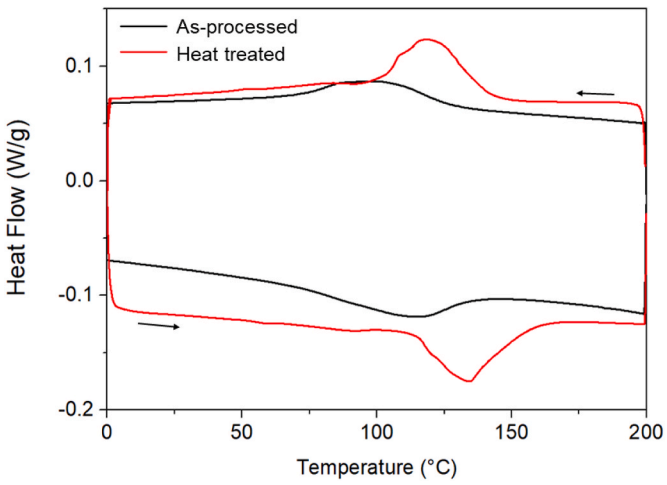

Fig. 3. Differential scanning calorimetry for the as-produced and heat treated NiMnGa samples. Exothermal direction: up.

partial sintering occurred, meaning that process parameters can be further optimized to achieve full density. From the observation of a series of cross sections of the as-produced sample (not reported in this

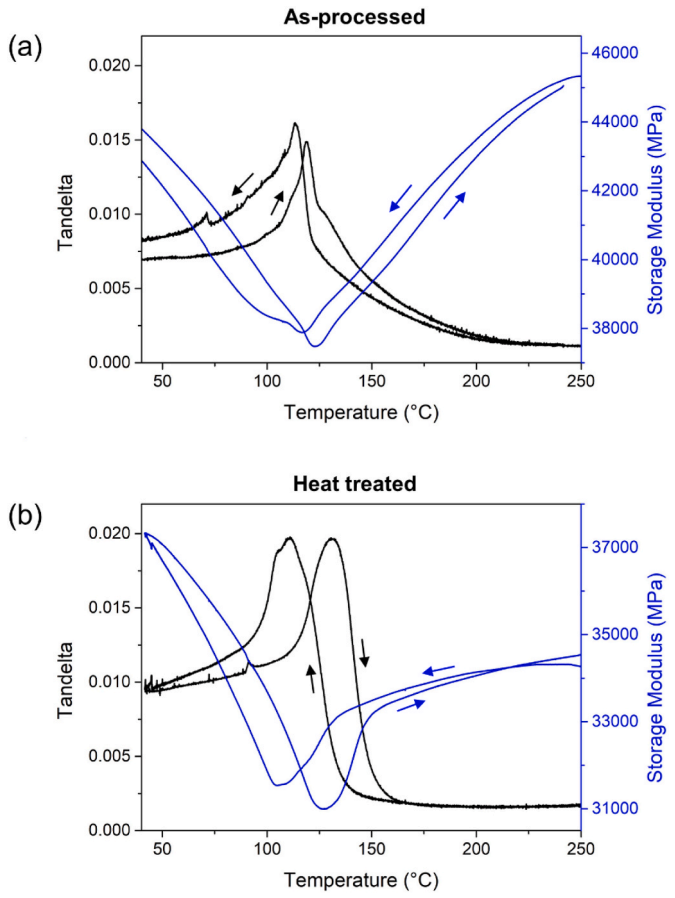

Fig. 4. Tan(δ) (black curve) and storage modulus (blue curve) obtained from the DMTA analysis on NiMnGa as-produced (a) and heat treated (b) samples.

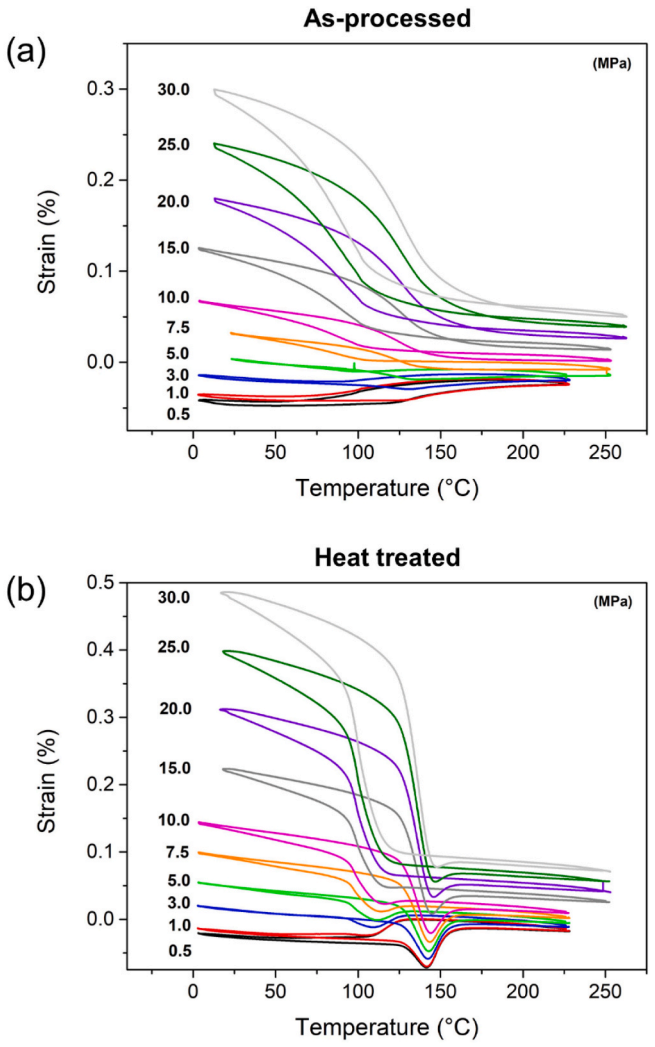

Fig. 5. Strain recovery curves upon fixed applied stresses on as-produced (a) and heat treated (b) NiMnGa alloy.

manuscript), it was possible to observe that porosity is preferentially distributed in the outer shell of the sample. Therefore, the specimens for the thermal and mechanical characterizations were cut from the core of the as-produced sample where almost full density was achieved. The microstructure of the as-produced and heat treated NiMnGa at higher magnification is reported in Fig. 2(c) and (d). Inside the compacted powders it is possible to identify different martensitic domains which are characterized by the typical twin structure. Moreover, the crystal domains and twins have not homogeneous sizes, particularly in the as-processed sample, and the boundaries between different crystal domains are clearly visible. Finally, some pores and oxides, which were identified as Mn-based ones by means of EDX analysis, are visible in the high magnification micrographs.

The calorimetric analysis was performed on the as-processed and heat-treated samples and the results are reported in Fig. 3. The heat treatment induces a shift of the martensitic transformation towards higher temperatures, with the increase of the A_f temperature from 134 °C to 154 °C. Moreover, the peaks related to the transformation are narrower for the heat-treated sample and this could be due to the homogenization of the microstructure. More specifically, the thermally-induced martensitic transformation is sharper in the case of the heat treated sample because the thermal energy required to induce the transformation of the whole material corresponds to a narrower range of temperatures. On the other hand, the as-produced material transforms over a wider range of temperatures because the transformation is hindered by a larger amount of energy barriers provided by the thermo-mechanical processing. The heat treatment allows the microstructural homogenization and therefore the partial release of these energy barriers stored at microstructural level that are generated by the interaction between defects, e.g. pores, oxides and dislocations, and grain structure. The same effect has been reported in Ref. [26]. In addition, with the heat treatment, the transformation enthalpy upon cooling increases from 6.0 J/g to 7.2 J/g meaning that the possible caloric effect of the alloy is enhanced. Indeed, according to the calorimetric-based approach for the evaluation of the caloric performance of shape memory alloys, the maximum achievable ΔT can be assessed through the ratio between the enthalpy related to the forward TMT and the specific heat of the alloy [40]. The specific heat was measured through modulated calorimetric measurements at 170 °C and the values were 0.39 and 0.26 J/(g°C) for the as-rolled and the heat-treated alloy, respectively. Therefore, the highest cooling and heating potential is expected for the heat treated NiMnGa sample and the maximum theoretical ΔT, i.e. ΔT_{DSC}, corresponds to 28 °C.

3.2. DMTA and strain recovery measurements

The results of the bending DMTA on the as-produced and heat treated NiMnGa samples are shown in Fig. 4. The tan*(δ)* trends (black curves) show the typical peak due to the sum of TMT and the transitory contributions [38,39]. The curve of the heat treated alloy presents a sharper trend in correspondence of the TMT, confirming the results of the calorimetric analysis. The peak value is 0.016 for the as-processed sample (Fig. 4(a)) and 0.019 for the heat treated one (Fig. 4(b)). The

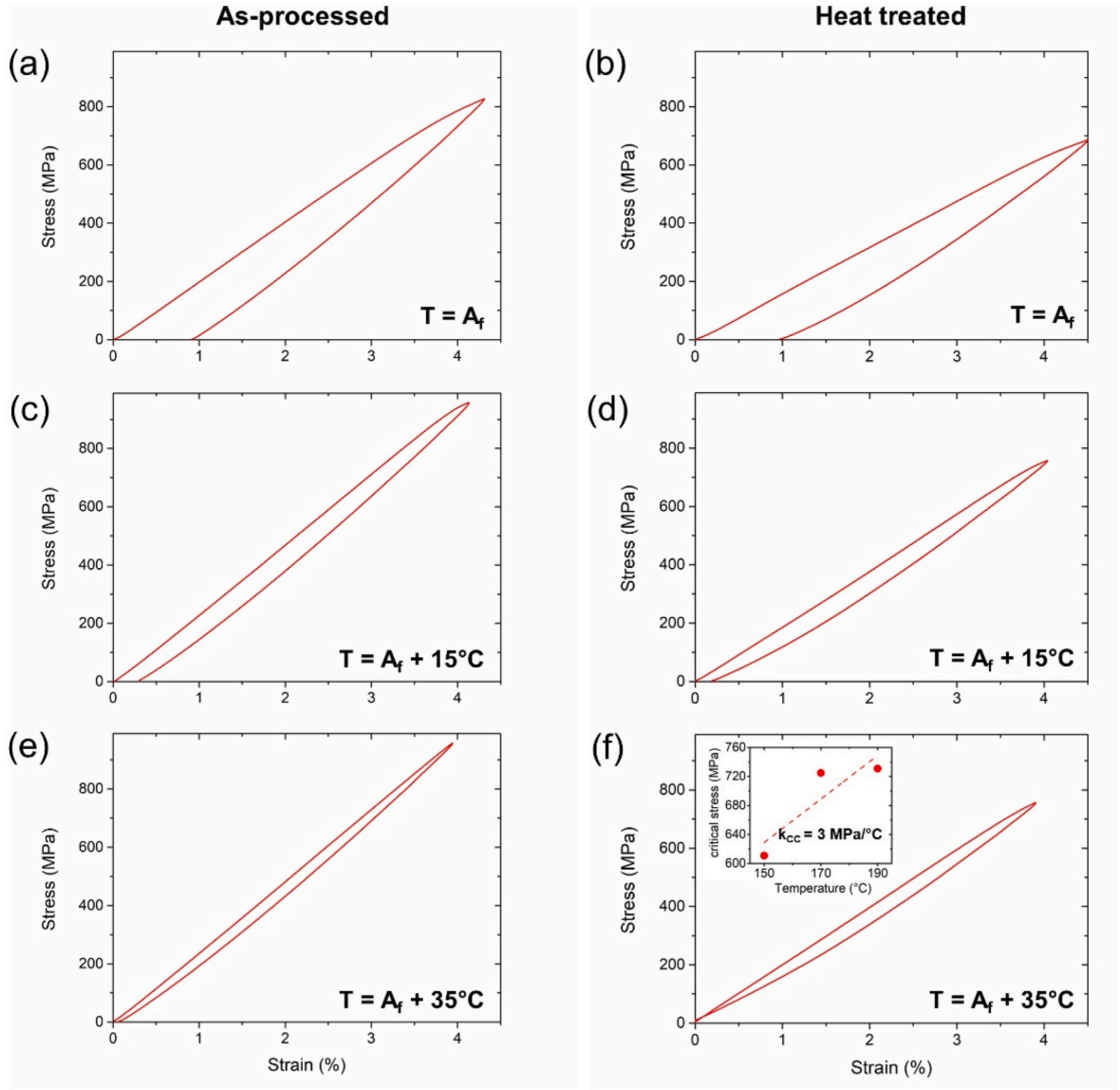

Fig. 6. Isothermal stress-strain curves for the as-processed and heat treated NiMnGa samples in austenite at different temperatures. The inset in (f) shows the critical stresses versus temperature derived from the austenitic curves of the heat-treated sample and the slope of their linear interpolation is indicated as k_{CC}.

intrinsic tan*(δ)* of the austenitic phase is 0.001 for both samples. The tan *(δ)* value for martensitic phase of the as-produced sample is between 0.007 and 0.008, while for the heat treated sample it reaches 0.009. As expected, the damping capacity of the martensite is higher than that of the austenite, since the low energy twin boundaries are highly mobile and efficient in dissipate vibrations [39,41]. However, the tan*(δ)* of the NiMnGa produced by rolling and heat treated in this work are one order of magnitude lower than the values typically registered for the cast alloy [16]. Indeed, the intergranular cracks observed in the cast NiMnGa alloy are responsible for further energy dissipation. Therefore, the lower number of microstructural defects in the material sintered by rolling is likely to have a positive effect on the structural integrity and ductility of the material.

The blue curves in Fig. 4 show are related to the storage modulus that ranges between 37.5 and 45.3 GPa and between 31 and 37.3 GPa in the investigated temperature range for the as-rolled and heat treated alloys respectively.

Another evidence of the increased elasticity of the sintered alloy was obtained from the strain recovery measurements reported in Fig. 5. The strain recovery tests investigated the evolution of the TMT with different applied stresses registering the recovered strain as a function of the temperature. It is possible to observe that by applying up to 30 MPa, the deformation is completely recovered both by the as-produced and heat-treated sample. Moreover, this measurement points out that the TMT of the heat treated alloy occurs in a sharper way and in a narrower temperature range with respect to the as-produced material. This is in good agreement with the results achieved by Ref. [26]. Finally, it is possible to observe that at low applied stresses, the alloy presents an inverse strain behavior which is visible up to 5 MPa and 3 MPa of applied stress for the as-produced and heat-treated sample, respectively. Indeed, the strain decreases during cooling, whereas it increases during heating. The same effect was observed in the NiMn-based melt spun ribbons. The authors attributed the inverse strain recovery to the effect of fast cooling induced by melt spinning which caused the formation of residual stresses [42]. Similarly, in NiMnGa alloy produced by powder metallurgy route (e.g. by ODP method [26] or sintering by hot-rolling as in this work), residual stresses might arise and be responsible of this effect. In this case, the processing is different because it consists in a mechanically- and thermally-aided powder compaction and residual stresses can be generated. Therefore, it is possible to assume that residual stresses with

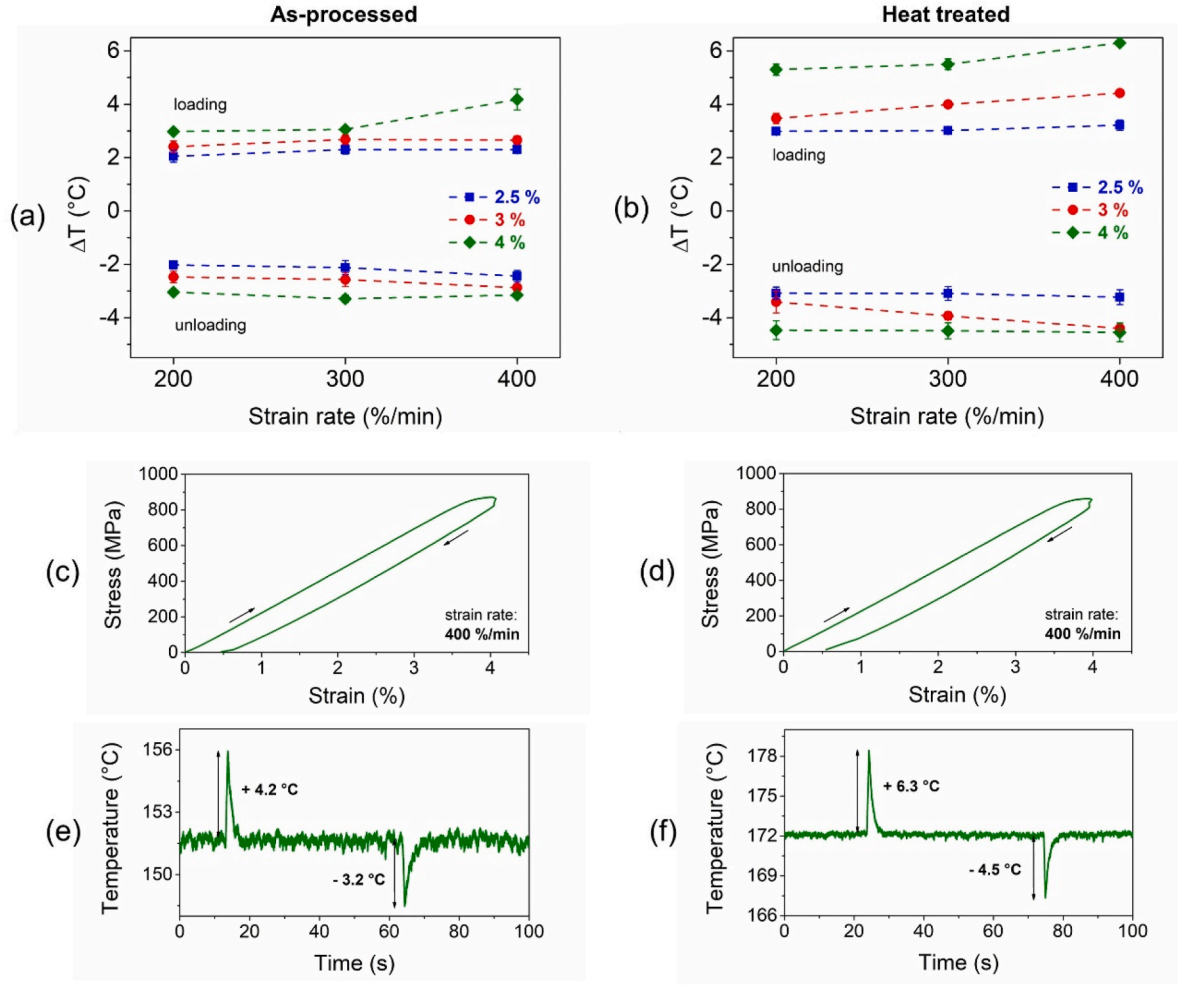

Fig. 7. Summary of the ΔT_{exp} obtained in different loading conditions for as-rolled (a) and heat treated (b) NiMnGa. The adiabatic stress-strain curves (c) and (d) and the related temperature profiles (e) and (f) for the best loading conditions of as-processed and heat treated samples.

different origins induce the same inverse strain recovery effect in ribbons and sintered NiMnGa samples. Moreover, this material feature is in accordance with the thermally-induced martensitic transformation analysis that evidenced a lower amount of energy barriers in the heat treated sample. The lower extent of inverse behavior exhibited by the heat treated alloy can be ascribed to the partial release of these residual stresses thanks to the thermal treatment itself, as similarly occurred in NiMnGa produced by ODP and heat treated [26]. Therefore, it is necessary a lower applied load to reach and overcome the internal stress and obtain a direct strain behavior.

3.3. Elastocaloric characterization

The assessment of the elastocaloric performance was carried out on the as-rolled and heat-treated samples. First of all, the isothermal characterization of the mechanical behavior of the samples in austenitic state was performed and the results are reported in Fig. 6.

It is possible to notice that the martensitic transformation is not sharply induced at a precise stress level and, therefore, a flat plateau is not visible. The same behavior was exhibited by the ODP sintered samples [27] and it can be ascribed to the highly elastic response discussed in section 3.2. For both samples, by increasing the temperature from *Af* to *Af* + 35 °C the hysteresis between loading and unloading phases is reduced. Moreover, the residual strains decrease from 1% at *Af* temperature to zero. In addition, the critical stresses for the martensite induction, identified in correspondence of the changes of slope of the loading curves estimated by the intersection of the tangent to the initial elastic and final part of the curve, increase. The estimation of the critical stresses of the as-processed sample at *Af* + 35 °C by the tangent method was not possible. However, the approximation of the critical stresses for the formation of martensite in the heat treated alloy are reported in the inset of Fig. 6(f) and the slope of the linear interpolation of the data is 3 MPa/°C. This latter parameter, called k_{CC}, is the Clausius-Clapeyron coefficient and represents the relation between the stress necessary to induce the martensitic transformation and the operating temperature, i.e. dσ/dT [43]. The obtained value is in accordance with a result achieved in a previous study [44]. The k_{CC} allows the estimation of the entropy change related to the stress-induced martensitic transformation according to the equation [45]:

$$|\Delta S| = \frac{1}{\rho} k_{CC} \Delta\varepsilon$$

where Δε is the recovered strain and ρ is the density of the alloy. For the heat treated NiMnGa, ΔS is equal to 15.6 J/(kg°C). In turn, the theoretical ΔT generated by the stress induced martensite is calculated according to the following equation [46]:

$$|\Delta T_{CC}| = \frac{T}{c_p} |\Delta S|$$

where T is the operating temperature and c_p is the specific heat. The ΔT_{CC} computed for the heat treated NiMnGa sample is 10.6 °C.

Table 1
Summary of the theoretical and experimental ΔT values for NiMnTi heat treated alloy.

	$\lvert\Delta T_{DSC}\rvert$	$\lvert\Delta T_{CC}\rvert$	$\lvert\Delta T_{exp}\rvert$
NiMnGa heat treated	28.0 °C	10.6 °C	6.3 °C

Table 2
Summary of the adiabatic DT obtained for NiMnGa alloys in recent works.

Alloy composition (in atomic %) and microstructure	Adiabatic ΔT	Reference
$Ni_{50}Mn_{30}Ga_{20}$ single crystal	12.3 °C	[33]
$Ni_{55}Mn_{18}Ga_{27}$ directionally solidified	10.7 °C	[34]
$Ni_{50.4}Mn_{27.3}Ga_{22.3}$ directionally solidified	6.5 °C	[35]
$Ni_{50}Mn_{30}Ga_{20}$ polycrystalline	3.5 °C	[47]
$Ni_{50}Mn_{30}Ga_{20}$ polycrystalline sintered (ODP)	4.0 °C	[27]
$Ni_{50}Mn_{30}Ga_{20}$ polycrystalline sintered (hot rolling of canned powders)	6.3 °C	This work

Finally, direct measurements of the ΔT generated during adiabatic loading and unloading cycles at $Af + 15$ °C were performed to assess the elastocaloric performance of the investigated material. In this way, the caloric performance of the produced alloy was determined experimentally. For each combination of applied strains and strain rates, five adiabatic cycles were carried out and the measured temperature spans (ΔT_{exp}) are summarized in Fig. 7(a) and (b). As expected, by increasing the applied strain, the achieved ΔT_{exp} is increased due to a higher fraction of transformed material. Moreover, the adiabatic condition is more closely approximated by increasing the strain rate since the heat transfer towards the environment is increasingly prevented. The best performance is given by the heat-treated NiMnGa upon an applied strain of 4 % and a strain rate of 400 %/min (Fig. 7(d)). These loading conditions lead to a ΔT_{exp} of +6.3 °C during loading and - 4.5 °C during unloading (Fig. 7(f)).

Table 1 presents a comparison between the different approaches used for the evaluation of the adiabatic ΔT in the heat-treated alloy. The theoretical value of ΔT evaluated from the calorimetric data (ΔT_{DSC}) is higher than the ΔT_{CC} because it is related to the total heat transfer associated with the thermally induced martensitic transformation, while the ΔT_{CC} is due to the stress-induced transformation. Indeed, the microstructural features of the alloy, i.e. grain boundaries, defects, or impurities, that are extensively present in these samples, can enhance the amount of energy required to induce the detwinned martensite by stress and decrease the estimated ΔT [40]. The maximum ΔT determined experimentally upon rapid loading and unloading cycles is 6.3 °C, being lower than the theoretical ones because the adiabatic conditions are not perfect and partial heat transfer to the environment occurs [27].

The elastocaloric performance of the sintered and heat-treated alloy, in terms of adiabatic ΔT, is significant for a polycrystalline NiMnGa. Moreover, the ΔT values achieved are slightly higher than those obtained in the same conditions for the same alloy produced by ODP [27].

Table 2 presents a comparison between various recently-developed NiMnGa alloys and the one studied in this work. In the current work, a cost-effective production route allowed to obtain NiMnGa samples which exhibited lower adiabatic ΔT than directionally solidified alloys or single crystals. However, these methods are costly and difficult to scale up to larger production scale for possible applications. At the same time, other polycrystalline NiMnGa exhibited lower ΔT. Therefore, the performance of the polycrystalline sintered NiMnGa in the current work is enhanced and promising for possible practical scopes.

4. Conclusions

The newly developed rolling-sintering process allowed the production of quasi fully dense $Ni_{50}Mn_{30}Ga_{20}$ (at. %) samples. The thermoelastic martensitic transformation temperatures of the as-produced alloy can be shifted and optimized by the application of a thermal treatment at 925 °C for 6 h that also allowed the enhancement of the transformation enthalpy, thus the cooling and heating potential of the alloy. The DMTA analysis and strain recovery measurements evidenced the prevalence of the elastic component of the material response when solicited by dynamic strains and the consequent brittleness reduction. Moreover, the inverse behavior exhibited by the strain recovery upon low loads was probably caused by the presence of residual stresses stored inside the produced samples. These internal stresses could be caused by the severe thermo-mechanical processing and they were partially released by the heat treatment. The characterization was completed through compressive mechanical tests that were carried out to assess the elastocaloric performance of the alloy in terms of adiabatic ΔT. Six combinations of applied strains and strain rates were adopted for the direct measurement of the ΔT during adiabatic loading and unloading cycles. The maximum achieved ΔT is 6.3 °C with an applied strain of 4 % and a strain rate of 400 %/min and this is a promising result for the assessment of the "rolling-sintering" as a suitable process for the NiMnGa production for elastocaloric applications.

Data availability

The data that support the findings of this study are available from the corresponding author upon reasonable request.

Declaration of competing interest

The authors declare that they have no known competing financial interests or personal relationships that could have appeared to influence the work reported in this paper.

Acknowledgments

The Authors are grateful to Nicola Bennato for the preparation of the NiMnGa ingots.

References

[1] Mendonça AA, Jurado JF, Stuard SJ, Silva LEL, Eslava GG, Cohen LF, Ghivelder L, Gomes AM. Giant magnetic-field-induced strain in Ni2MnGa-based polycrystal. J Alloys Compd 2018;738:509–14.
[2] Chernenko VA, L'vov VA. Magnetoelastic nature of ferromagnetic shape memory effect. Mater Sci Forum 2008;583:1–20.
[3] Albertini F, Solzi M, Paoluzi A, Righi L. Magnetocaloric properties and magnetic anisotropy by tailoring phase transitions in NiMnGa alloys. Mater Sci Forum 2008; 583:169–96.
[4] Villa E, Tomasi C, Nespoli A, Passaretti F, Lamura G, Canepa FJ. Investigation of microstructural influence on entropy change in magnetocaloric polycrystalline samples of NiMnGaCu ferromagnetic shape memory alloy. Mater. Res. Technol. 2020;9:2259–66.
[5] Karaca HE, Karaman I, Basaran B, Lagoudas DC, Chumlyakov YI, Maier HJ. On the stress-assisted magnetic-field-induced phase transformation in Ni2MnGa ferromagnetic shape memory alloys. Acta Mater 2007;55:4253–69.
[6] Ullakko K, Huang JK, Kantner C, O'Handley RC, Kokorin VV. Large magnetic-field-induced strains in Ni2MnGa single crystals. Appl Phys Lett 1996;69:1966–8.
[7] Planes A, Stern-Taulats E, Castán T, Vives E, Mañosa L, Saxena A. Caloric and multicaloric effects in shape memory. Alloys Materials Today: Proceedings 2015;2 (S3):S477–84.
[8] Pfeuffer L, Gràcia-Condal A, Gottschall T, Koch D, Faske T, Bruder E, Lemke J, Taubel A, Ener S, Scheibel F, Durst K, Skokov KP, Mañosa L, Planes A, Gutfleisch O. Influence of microstructure on the application of Ni-Mn-In Heusler compounds for multicaloric cooling using magnetic field and uniaxial stress. 8 Acta Materialia 2021;217:117157.
[9] Besseghini S, Villa E, Passaretti F, Pini M, Bonfanti F. Plastic deformation of NiMnGa polycrystals. Mater Sci Eng 2004;378:415–8.
[10] Tanimura H, Tahara M, Inamura T, Hosoda H. Compressive fracture behavior of Bi-added Ni50Mn28Ga22 ferromagnetic shape memory alloys. MRS Online Proc Libr 2013;1516:139–44.
[11] Chernenko VA, Villa E, Salazar D, Barandiaran JM. Large tensile superelasticity from intermartensitic transformations in Ni49Mn28Ga23 single crystal. Appl Phys Lett 2016;108:071903.

[12] Wu GH, Yu CH, Meng LQ, Chen JL, Yang FM, Qi SR, Zhan WS, Wang Z, Zheng YF, Zhao LC. Giant magnetic-field-induced strains in Heusler alloy NiMnGa with modified composition. Appl Phys Lett 1999;75:2990–2.
[13] Surikov NY, Panchenko EY, Timofeeva EE, Tagiltsev AI, Chumlyakov YuI. Orientation dependence of elastocaloric effect in Ni50Mn30Ga20 single crystals. J Alloys Compd 2021;880:160553.
[14] Albertini F, Besseghini S, Paoluzi A, Pareti L, Pasquale M, Passaretti F, Sasso CP, Stantero A, Villa E. Structural, magnetic and anisotropic properties of Ni2MnGa melt-spun ribbons. J Magn Magn Mater 2002;242–245:1421–4.
[15] Vallal Peruman K, Vinodh Kumar S, Pushpanathan K, Mahendran M. Structural and martensitic transformation of bulk, disordered and nanocrystalline Ni2MnGa alloys. Funct. Mater. Lett. 2011;4:415–8.
[16] Villa F, Nespoli A, Fanciulli C, Passaretti F, Villa E. Physical characterization of sintered NiMnGa ferromagnetic shape memory alloy materials, vol. 13; 2020. p. 4806.
[17] Gao P, Tian B, Xu J, Tong Y, Li L. Microstructure, phase transformation and mechanical property of porous NiMnGa alloys prepared by one-step sintering. Mater Sci Eng, A 2020;788:139583.
[18] Taylor SL, Shah RN, Dunand DC. Ni-Mn-Ga micro-trusses via sintering of 3D-printed inks containing elemental powders. Acta Mater 2018;143:20–9.
[19] Caputo MP, Solomon CV. A facile method for producing porous parts with complex geometries from ferromagnetic Ni-Mn-Ga shape memory alloys. Mater Lett 2017;200:87–9.
[20] Caputo MP, Berkowitz AE, Armstrong A, Müllner P, Solomon CV. 4D printing of net shape parts made from Ni-Mn-Ga magnetic shape-memory alloys. Addit Manuf 2018;21:579–88.
[21] Taylor SL, Shah RN, Dunand DC. Microstructure and porosity evolution during sintering of Ni-Mn-Ga wires printed from inks containing elemental powders. Intermetallics 2019;104:113–23.
[22] Laitinen V, Sozinov A, Saren A, Chmielus M, Ullakko K. Characterization of as-built and heat-treated Ni-Mn-Ga magnetic shape memory alloy manufactured via laser powder bed fusion. Addit Manuf 2021;39:101854.
[23] Mostafaei A, Kimes KA, Stevens EL, Toman J, Krimer YL, Ullakko K, Chmielus M. Microstructural evolution and magnetic properties of binder jet additive manufactured Ni-Mn-Ga magnetic shape memory alloy foam. Acta Mater 2017;131:482–90.
[24] Mostafaei A, De Vecchis PR, Stevens EL, Chmielus M. Sintering regimes and resulting microstructure and properties of binder jet 3D printed Ni-Mn-Ga magnetic shape memory alloys. Acta Mater 2018;154:355–64.
[25] Dunand DC, Müllner P. Size effects on magnetic actuation in Ni-Mn-Ga shape memory alloys. Adv Mater 2011;23:216–32.
[26] Villa Francesca, Morlotti Andrea, Fanciulli Carlo, Passaretti Francesca, Albertini Franca, Villa Elena. Anomalous mechanical behavior in NiMnGa alloy sintered through open die pressing method. Mater Today Commun 2023;34:105391.
[27] Villa F, Tamandi M, Passaretti F, Bassani E, Villa E. Promising elastocaloric properties of sintered polycrystalline NiMnGa produced by open die pressing. J Mater Sci 2023;58(38):1–11.
[28] Manosa L, Planes A. Solid-state cooling by stress: a perspective. Appl Phys Lett 2020;116:050501.
[29] Moya X, Mathur ND. Caloric materials for cooling and heating. Science 2020;370:797–803.
[30] Takeuchi I, Sandeman K. Solid-state cooling with caloric materials. Phys Today 2015;68(12):48–54.
[31] Manosa L, Planes A. Materials with giant mechanocaloric effects: cooling by strength. Adv Mater 2017;29:1603607.
[32] Tušek J, Engelbrecht K, Manosa L, Vives E, Pryds N. Understanding the thermodynamic properties of the elastocaloric effect through experimentation and modelling. Shape Mem Superelast 2016;2:317–29.
[33] Surikov NY, Panchenko EY, Timofeeva EE, Tagiltsev AI, Chumlyakov YuI. Orientation dependence of elastocaloric effect in Ni50Mn30Ga20 single crystals. J Alloys Compd 2021;880:160553.
[34] Li D, Li Z, Yang J, Li Z, Yang B, Yan H, Wang D, Hou L, Li X, Zhang Y, Esling C, Zhao X, Zuo L. Large elastocaloric effect driven by stress-induced two-step structural transformation in a directionally solidified Ni55Mn18Ga27 alloy. Scripta Mater 2019;163:116–20.
[35] Wei L, Zhang X, Liu J, Geng L. Orientation dependent cyclic stability of the elastocaloric effect in textured Ni-Mn-Ga alloys. AIP Adv 2018;8:055312.
[36] Li D, Zhang X, Zhang G, Li Z, Yang B, Yan H, Wang D, Zhao X, Zuo L. Enhancing the elastocaloric effect in Ni–Mn–Ga alloys through the coupling of magnetic transition and two-step structural transformation. Appl Phys Lett 2021;118:213903.
[37] Li D, Li Z, Zhang X, Liu C, Zhang G, Yang J, Yang B, Yan H, Cong D, Zhao X, Zuo L. Giant elastocaloric effect in Ni-Mn-Ga-based alloys boosted by a large lattice volume change upon the martensitic transformation. ACS Appl Mater Interfaces 2022;14:1505–18.
[38] Villa F, Villa E, Nespoli A, Passaretti F. Internal friction parameter in shape memory alloys: correlation between thermomechanical conditions and damping properties in NiTi and NiTiCu at different temperatures. J Mater Eng Perform 2021;30:2605–16.
[39] San Juan J, Nó ML. Damping behavior during martensitic transformation in shape memory alloys. J Alloys Compd 2003;355:65–71.
[40] Villa F, Bestetti E, Frigerio R, Caimi M, Tomasi C, Passaretti F, Villa E. Elastocaloric properties of polycrystalline samples of NiMnGaCu ferromagnetic shape memory alloy under compression: effect of improvement of thermoelastic martensitic transformation. Materials 2022;150:7123.
[41] Liu Y, van Humbeeck J. On the damping behaviour of NiTi shape memory alloy. J. Phys. IV France 7 Proceedings 1997;7(C5). C5-C519-C5-524.
[42] Wójcik A, Aguilar-Ortiz C, Maziarz W, Szczerba MJ, Sikora M, ˙Zywczak A, Álvarez-Alonso P, Villa E, Flores-Zúniga H, Cesari E, Chernenko VA. Transformation behavior and inverse caloric effects in magnetic shape memory Ni44-xCuxCo6Mn39Sn11 ribbons. J Alloys Compd 2017;721:172–81.
[43] Moya X, Kar-Narayan S, Mathur ND. Caloric materials near ferroic phase transitions. Nat Mater 2014;13:439–50.
[44] Chernenko VA, Villa E, Salazar D, Barandiaran JM. Large tensile superelasticity from intermartensitic transformations in Ni49Mn28Ga23 single crystal. Appl Phys Lett 2016;108(7):071903.
[45] Bonnot E, Romero R, Manosa L, Vives E, Planes A. Elastocaloric effect associated with the martensitic transition in shape-memory alloys. Phys Rev Lett 2008;100:125901.
[46] Pataky GJ, Ertekin E, Sehitoglu H. Elastocaloric cooling potential of NiTi, Ni2FeGa and CoNiAl. Acta Mater 2015;96:420–7.
[47] Wei L, Zhang X, Gan W, Ding C, Geng L. Hot extrusion approach to enhance the cyclic stability of elastocaloric effect in polycrystalline Ni-Mn-Ga alloys. Scripta Mater 2019;168:28–32.